Nuclear clusters in low-energy nuclear reaction and neutron- star crust

Takashi Nakatsukasa

Center for Comp. Sci., Univ. of Tsukuba

- Quantum clusters
- Low-energy nuclear reaction
  - Reaction path, Inertial mass
- Neutron-star crust
  - Pasta phase, Entrainment effect

2019.5.31-6.1「第二回クラスター階層領域研究会」 @Tokyo Inst. Tech.

Quantum clusters

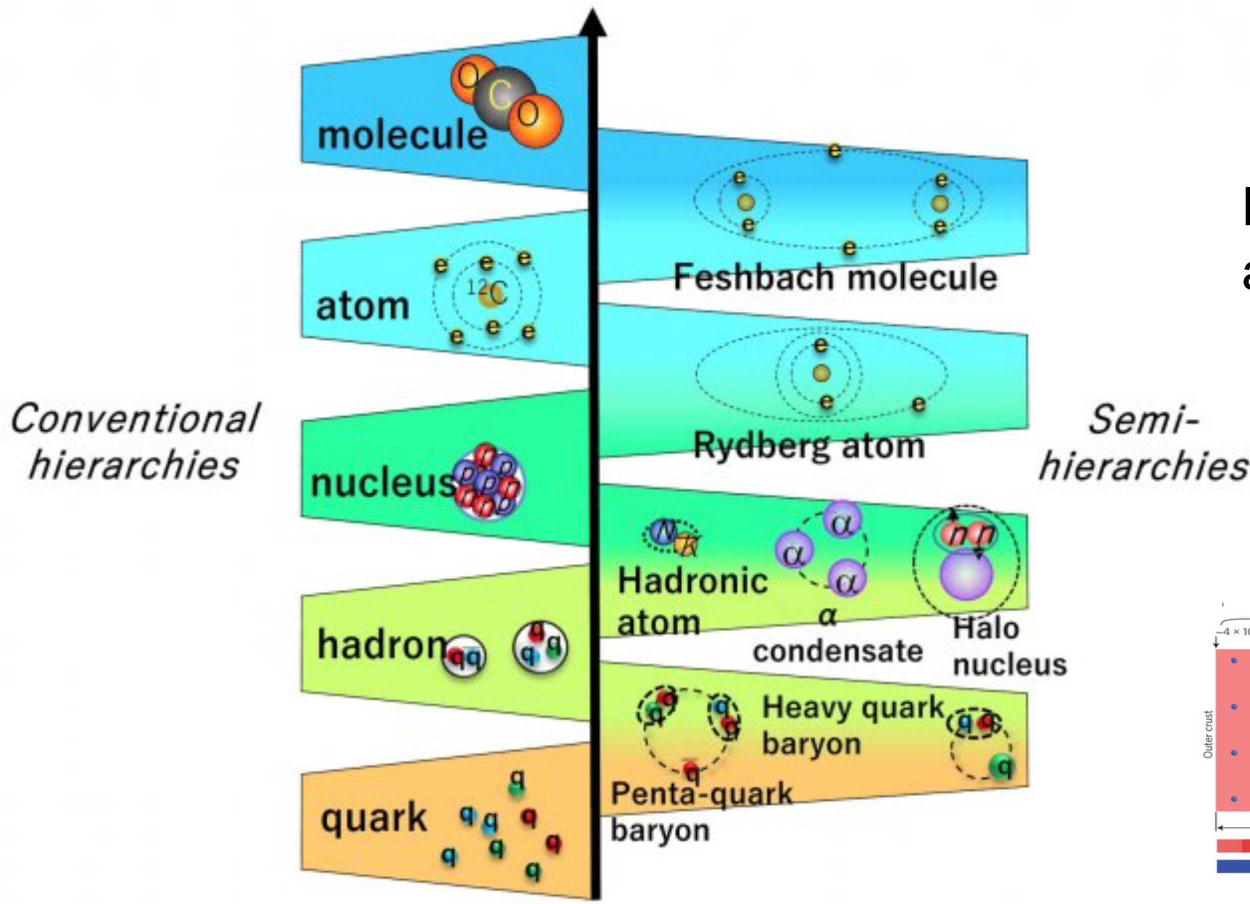

“Classical” “Quantum”

Nuclear deformation and clustering

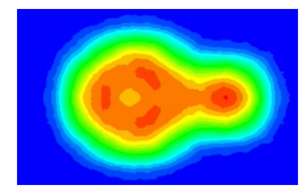

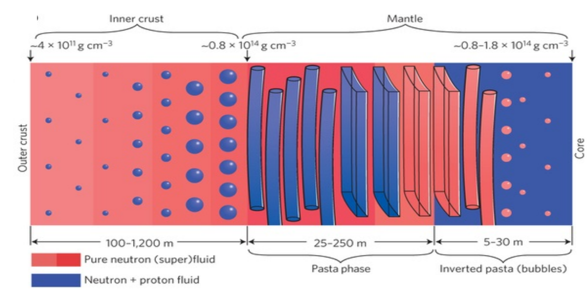

Inner crust of N$_{☆}$

Importance of quantum fluctuation

alpha-alpha potential

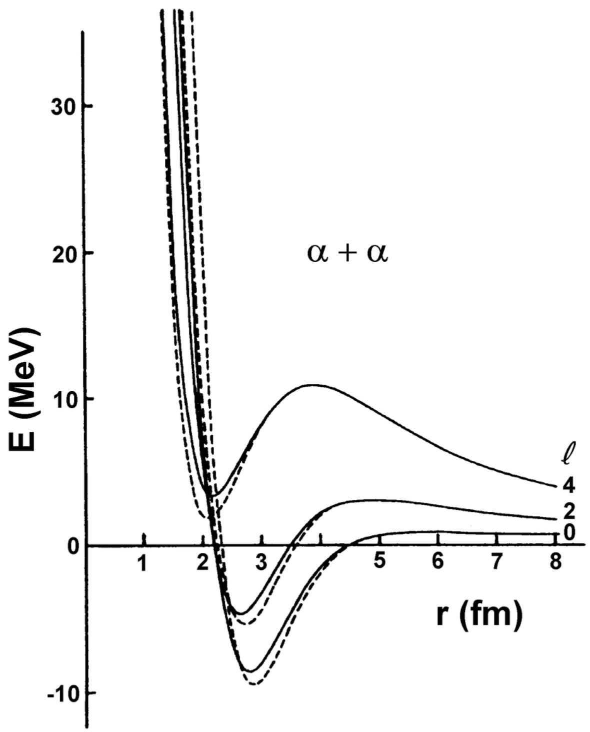

Spherical velocity distribution

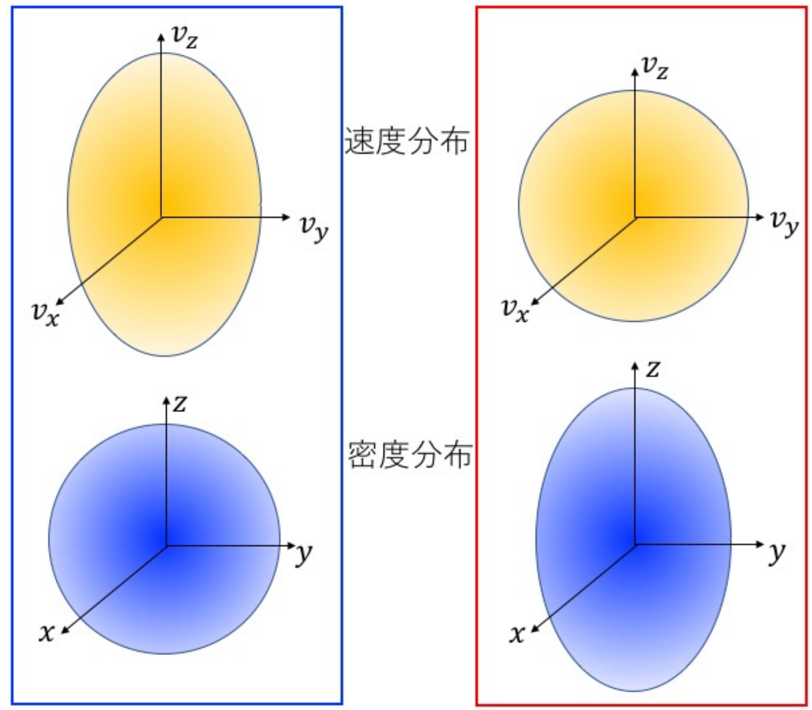

Academist journal (2019)

Minimal kinetic energy → Infinite uniform matter
Maximal attractive interaction → Finite nucleus

⇨

Nuclear deformation
Clustering

Neutron stars matter

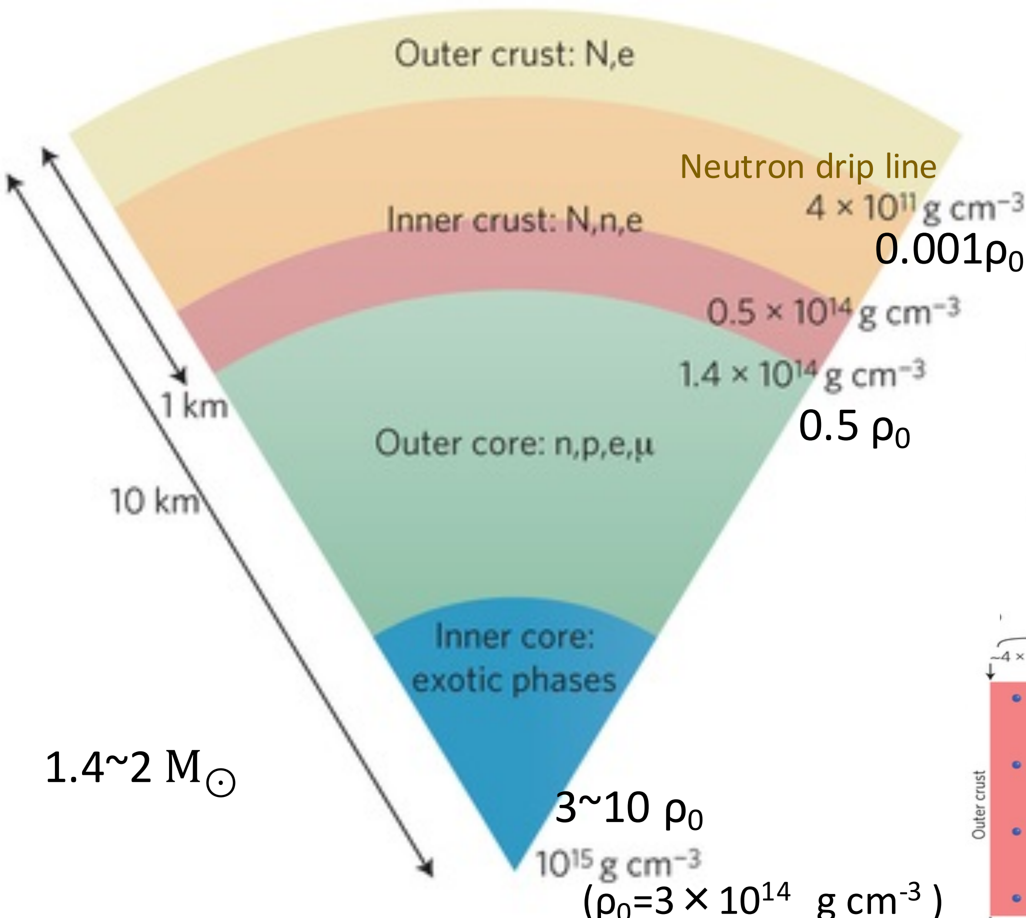

William G. Newton (2013)

- **Inner crust**

Neutron rich Nuclei

+ low-density neutrons gas

+ electrons gas

Toward accurate description of inner crust

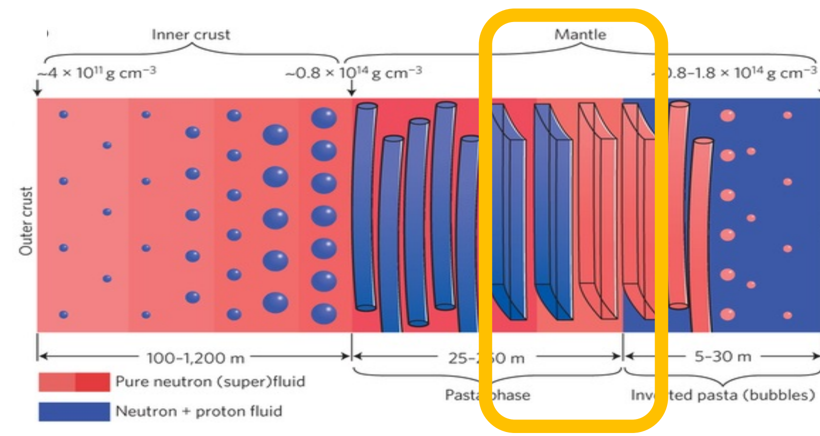

Nuclear Landscape

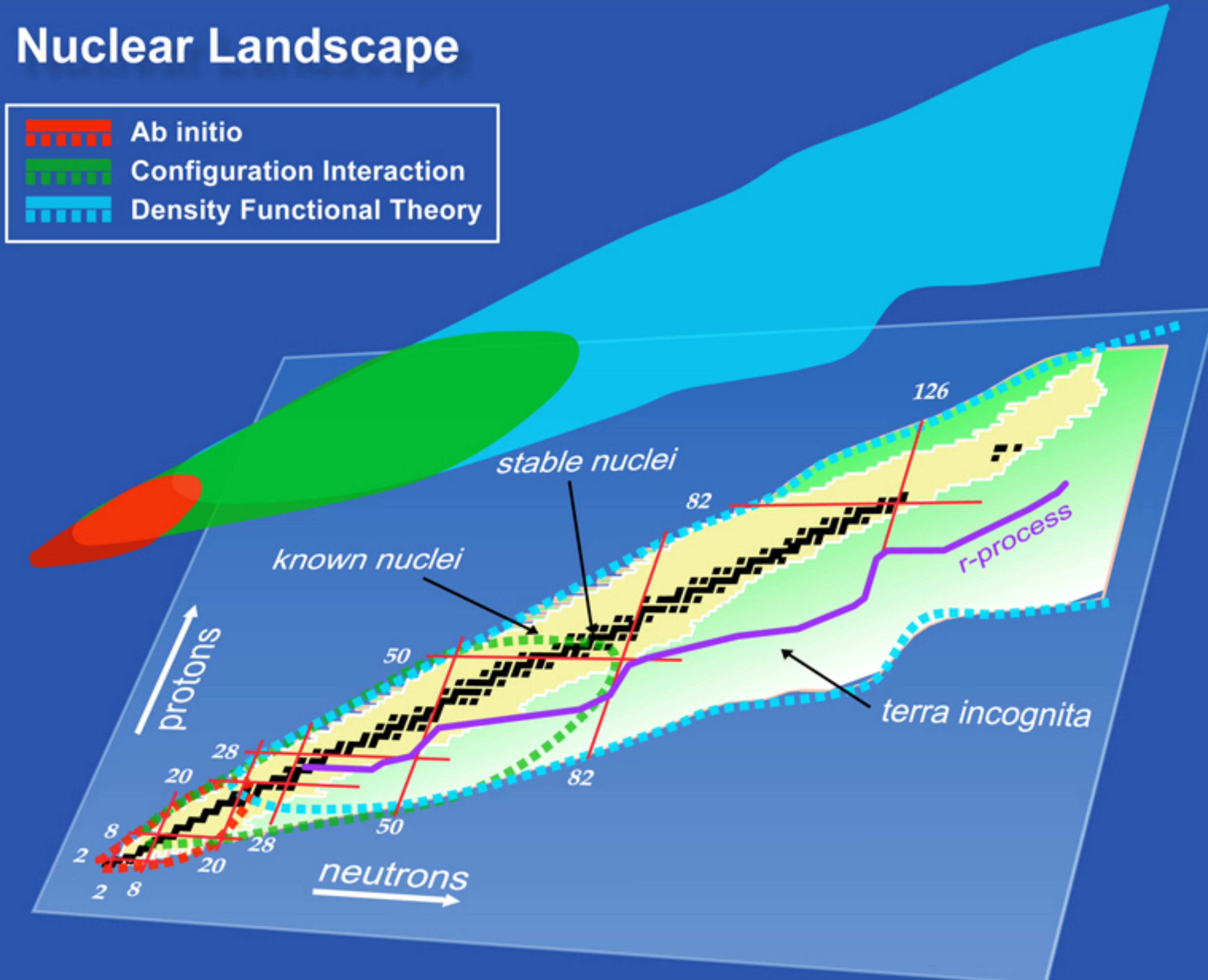

Self-consistent band calculation

- Periodic potential along z axis

  V(z + a)=V(z)

- KS equation :

$$h_k[\rho]\phi_{k,i}(z) = \varepsilon_{k,i}\phi_{k,i}(z)$$

$$h_k[\rho] = \frac{(p_z + k)^2}{2m} + V_{KS}[\rho]$$

$$\phi_{k,i}(z + a) = \phi_{k,i}(z)$$

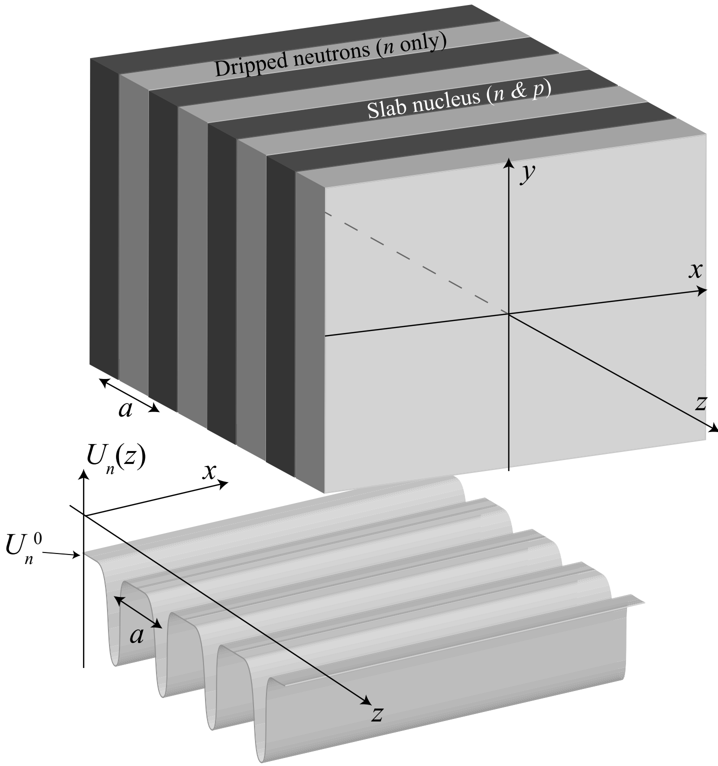

Number of k = Number of unit cells

In the present cal. we adopt 30 points for k.

Validity of TF approx.

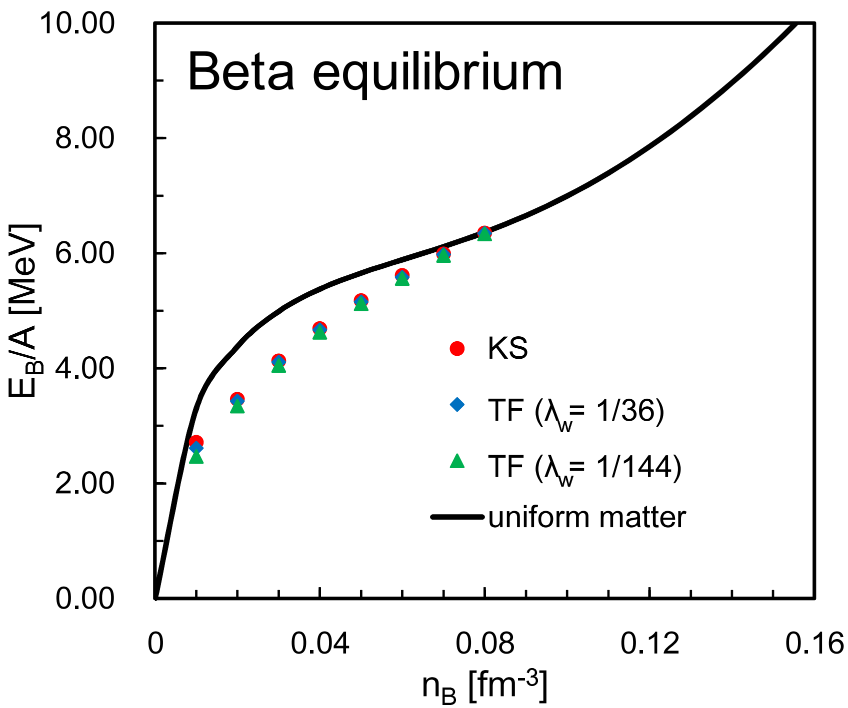

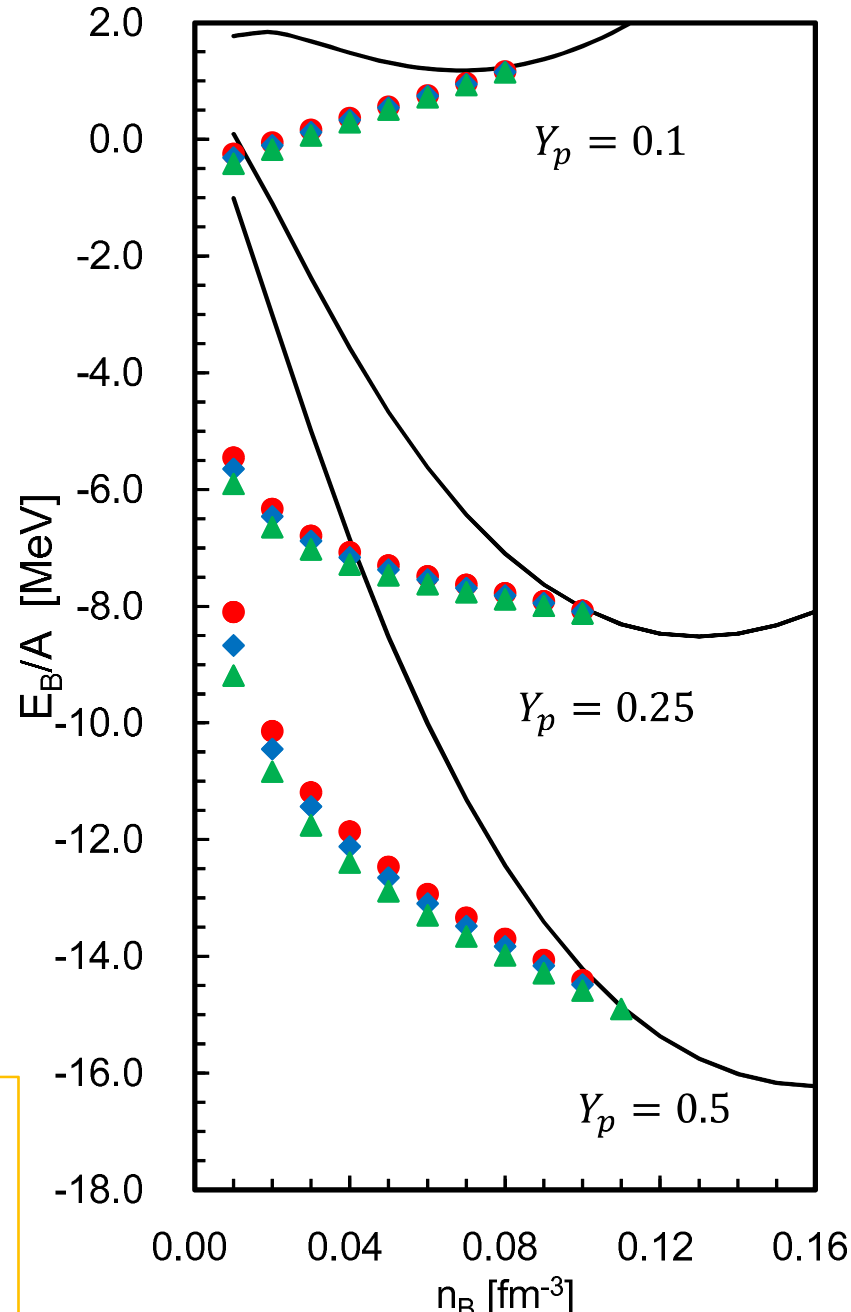

TF approx.:
Good at beta equilibrium
Bad at low density and high Y_p

Density profiles

$Y_p = 0.25$

$\rho_B = 0.02\ \mathrm{fm}^{-3}$

$a \approx 40$ fm (TF)
$a \approx 50$ fm (Band)

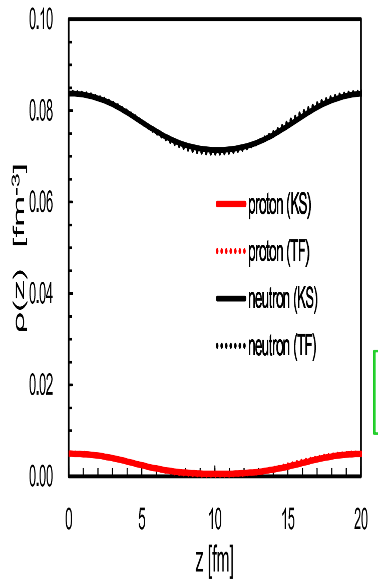

Beta equilibrium
$\rho_B = 0.08\ \mathrm{fm}^{-3}$

Anti-slab phase

$a \approx 20$ fm

$a \approx 20$ fm

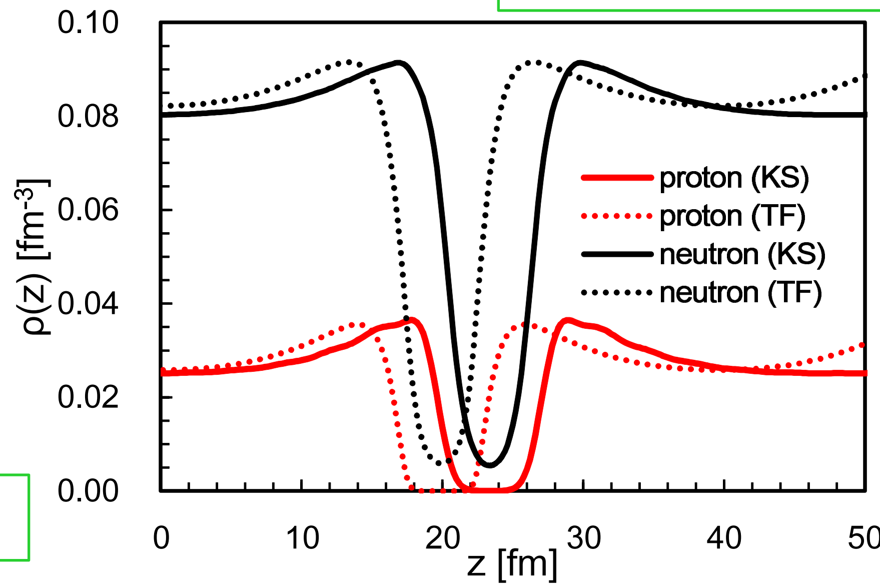

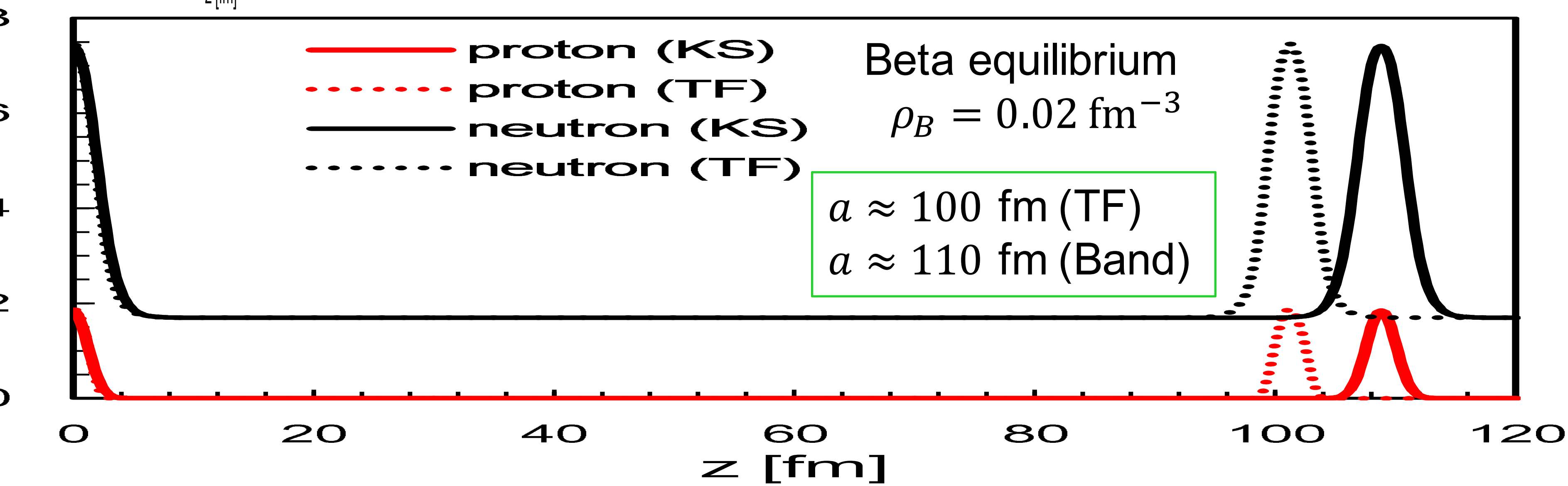

Beta equilibrium
$\rho_B = 0.02\ \mathrm{fm}^{-3}$

$a \approx 100$ fm (TF)
$a \approx 110$ fm (Band)

Band calculation

Kashiwaba and Nakatsukasa, JPS Conf. Proc. 14, 020801 (2017)

$\rho_B = 0.04\ \mathrm{fm}^{-3}$ $\mu_n = 8.45$ MeV
(beta equilibrium) $a = 56.4$ fm

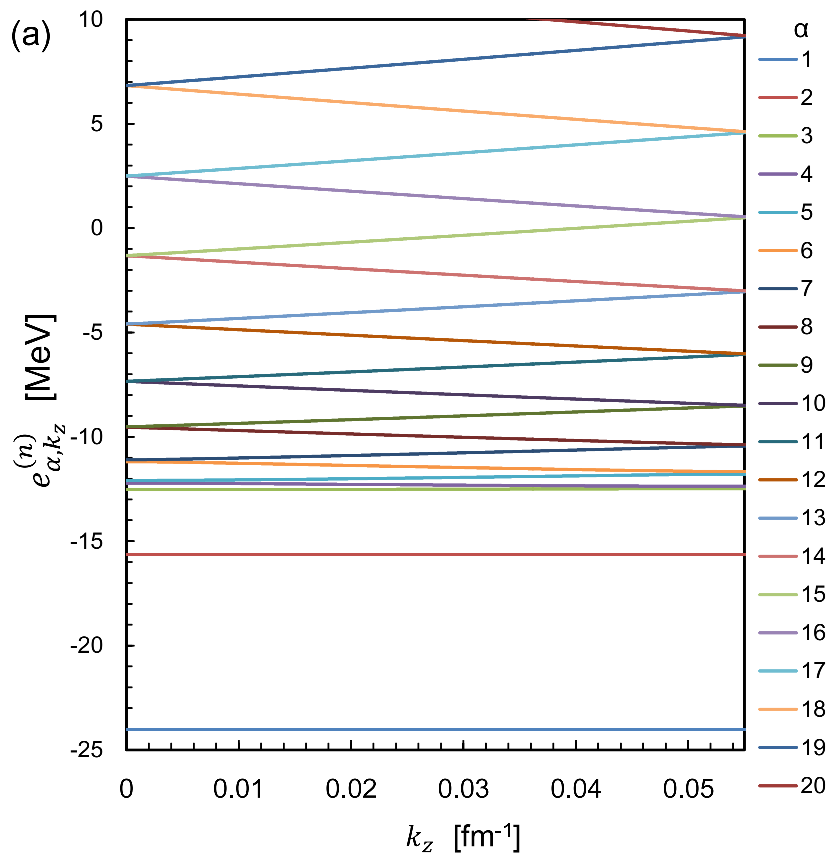

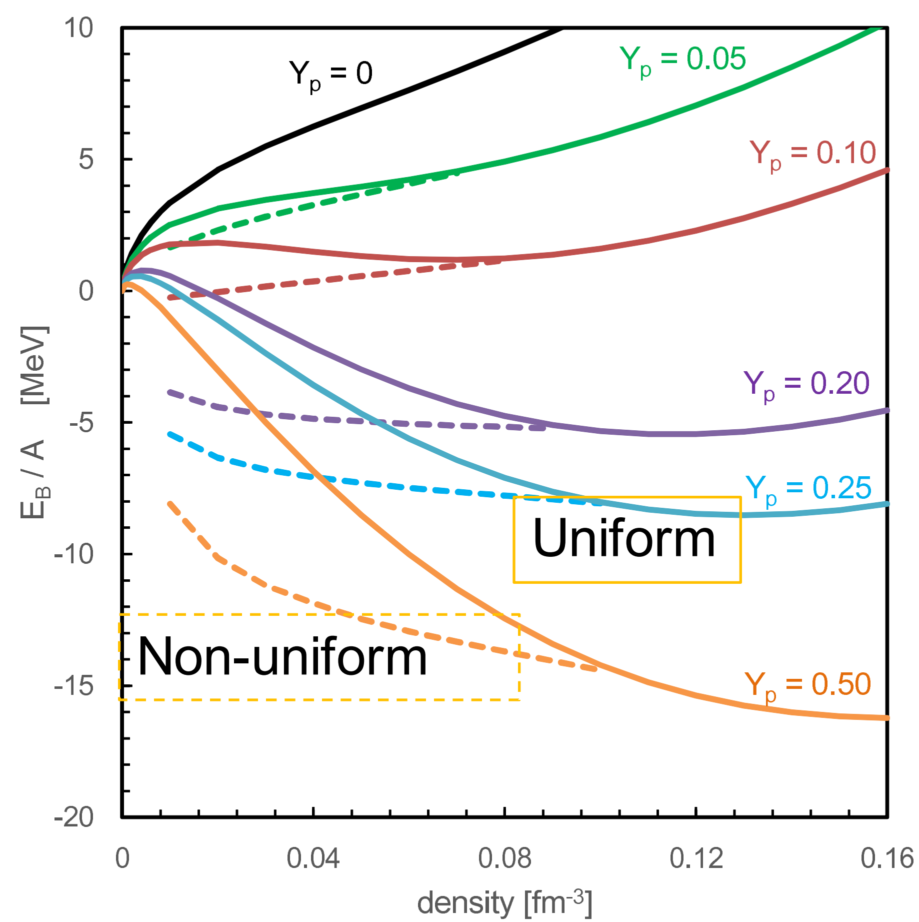

Effective mass for neutrons

Chamel, PRC 85, 035801 (2012)

$$\left(\frac{1}{m_n^*(\boldsymbol{k})^\alpha}\right)_{ij} = \frac{1}{\hbar^2}\frac{\partial^2 \varepsilon_{\alpha\boldsymbol{k}}}{\partial k_i \partial k_j},$$

$$n_n^{\mathrm{c}} = \frac{1}{3}\sum_\alpha \int \frac{d^3k}{(2\pi^3)}\tilde{n}^0_{\alpha\boldsymbol{k}}\,\mathrm{Tr}\left[\frac{m_n}{m_n^*(\boldsymbol{k})^\alpha}\right]$$

$$m_n^\star = m_n \frac{n_n^{\mathrm{f}}}{n_n^{\mathrm{c}}}.$$

Effective mass larger than 10 times more!

TABLE I. Composition of the inner crust of cold nonaccreting neutron stars as obtained from Ref. [2]. Z and A are, respectively, the average number of protons and the *total* average number of nucleons inside the Wigner-Seitz cell. n_n is the average neutron density, n_n^{f} is the density of free neutrons as defined by the quantity ρ_{Bn} in Ref. [2], n_n^{c} is the density of conduction neutrons, and $m_n^\star$ is the neutron effective mass. Note that in the densest layer, $n_n^{\mathrm{f}} > n_n$ due to the formation of bubbles as indicated in Fig. 1.

$\bar{n}$ (fm^{-3})	Z	A	n_n^{f}/n_n (%)	$n_n^{\mathrm{c}}/n_n^{\mathrm{f}}$ (%)	$m_n^\star/m_n$
0.0003	50	200	20.0	82.6	1.21
0.001	50	460	68.6	27.3	3.66
0.005	50	1140	86.4	17.5	5.71
0.01	40	1215	88.9	15.5	6.45
0.02	40	1485	90.3	7.37	13.6
0.03	40	1590	91.4	7.33	13.6
0.04	40	1610	88.8	10.6	9.43
0.05	20	800	91.4	30.0	3.33
0.06	20	780	91.5	45.9	2.18
0.07	20	714	92.0	64.6	1.55
0.08	20	665	104	64.8	1.54

Observational constraints

Andersson et al., PRL 109 241103 (2012)

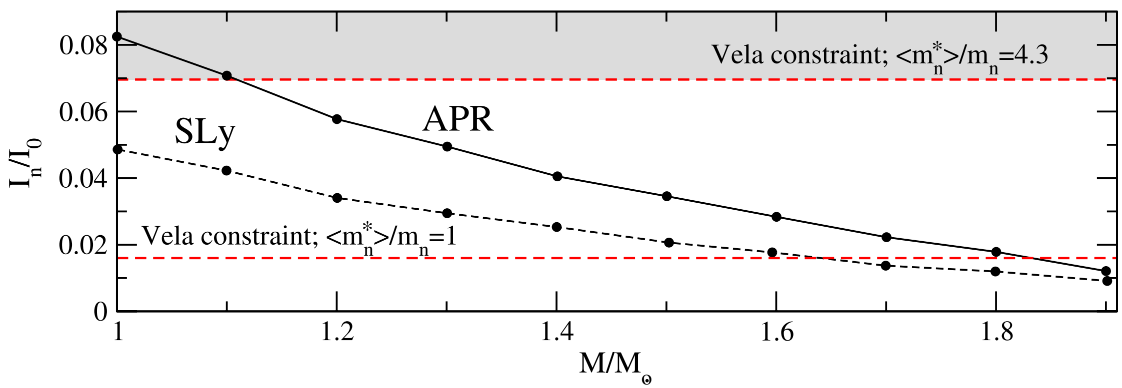

FIG. 3 (color online). The moment of inertia ratio I_n/I_0 as a function of the stellar mass for the models from Ref. [15] (APR) and Ref. [22] (SLy). If the glitches in the Vela pulsar are to be explained by the crust superfluid alone, then the moment of inertia ratio must satisfy $I_n/I_0 \gtrsim 0.016 \times (\langle m_n^* \rangle / m_n) \approx 0.07$ (gray region, with entrainment according to Ref. [10]; we also show the constraint when entrainment is not accounted for, as in Ref. [7].)

$$I_n \approx \frac{8\pi}{3} \int_{R_c}^{R} r^4 e^{(\lambda-\nu)/2} n_n \mu_n dr,$$

R_c: Crust-core interface
μ_n: Neutron chemical pot.
n_n: Free neutron density

Average value:

$$\frac{m_n^*}{m_n} \sim 4.3 - 4.4$$

Crust does not have enough neutrons to explain the glitches in the Vela pulsar.

Effective mass

Kashiwaba and Nakatsukasa, arXiv: 1904.10712

Mobility coef. $K^{zz} = 2\sum_{\alpha}\int \frac{d^3k}{(2\pi)^3}\frac{d^2\varepsilon_{\alpha k}}{dk_z^2}\theta(\mu_n - \varepsilon_{\alpha k})$

Effective mass $m^* = n/K^{zz}$

Near the bottom of the pasta phase

$$\frac{m^*}{m_n} \approx 0.7$$

Effective mass vs baryon density

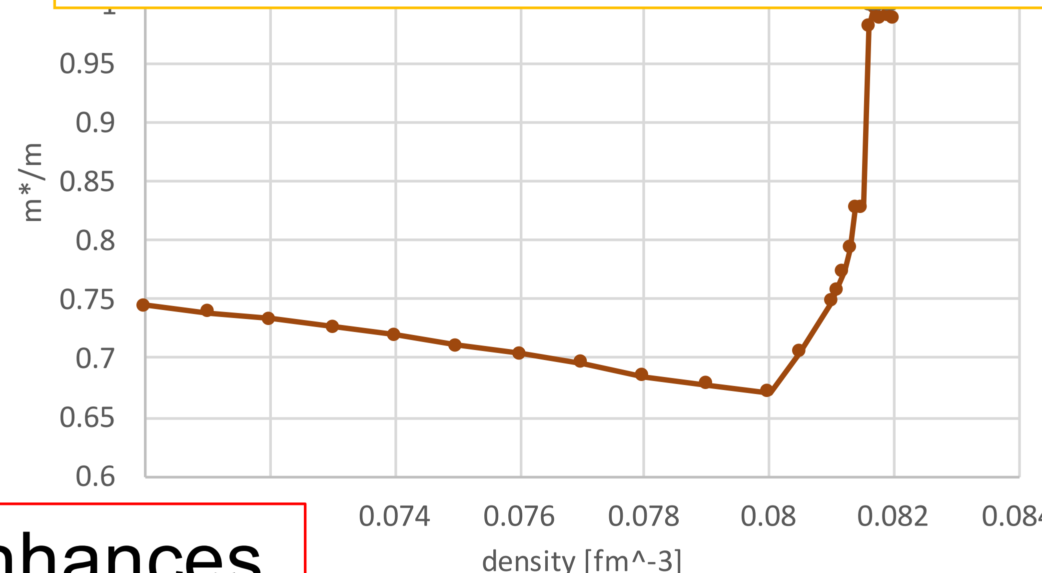

The Bragg scattering enhances mobility of dripped neutrons.

Emergence of cluster/pasta phase

- What kind of phases appear?
- Dynamical clustering, crust heating
- Finite-temperature effect
- Effect of neutron sea and superfluidity

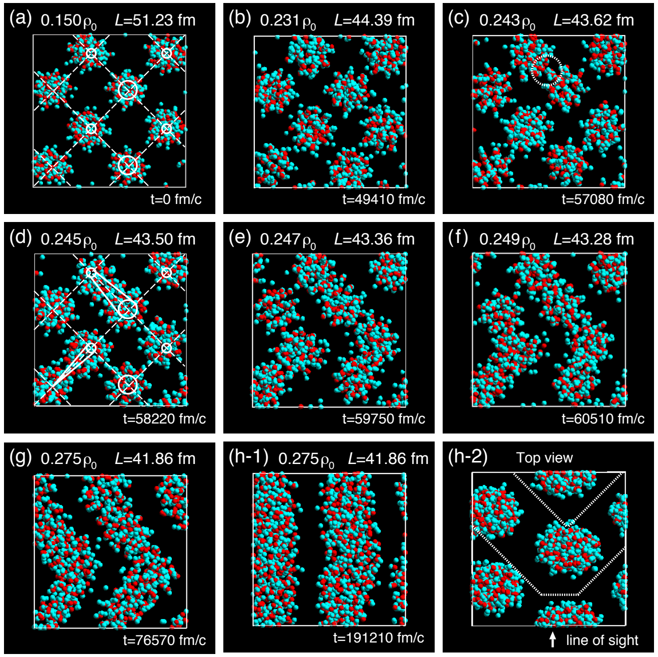

Watanabe et al., PRL (2009)

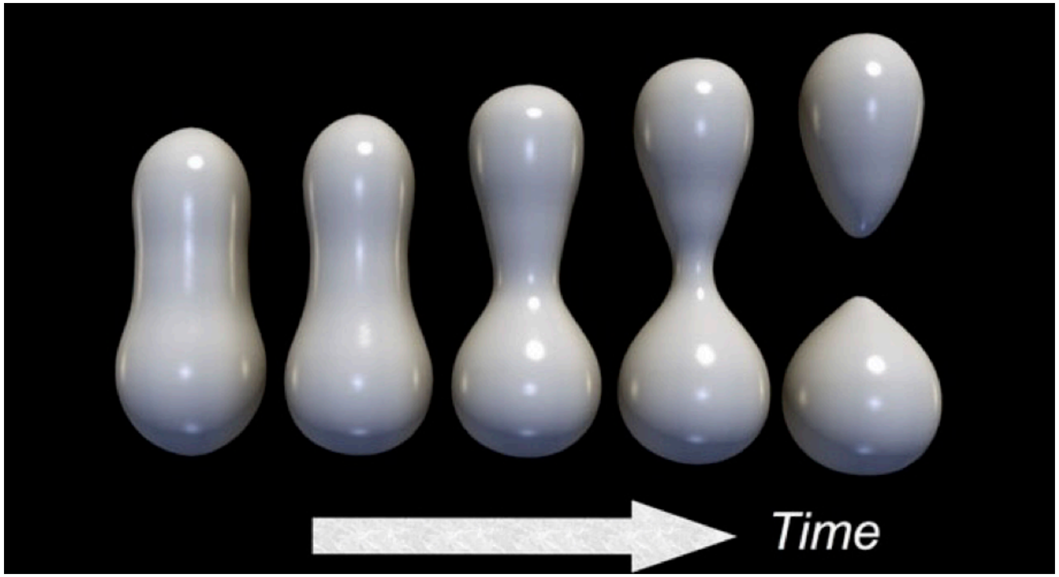

Scamps et al., Nature (2018)

Nuclear reaction and collective motion

- Nuclear decay
  - Spontaneous fission
  - Alpha decay
- Low-energy nuclear reaction
  - Sub-barrier fusion reaction

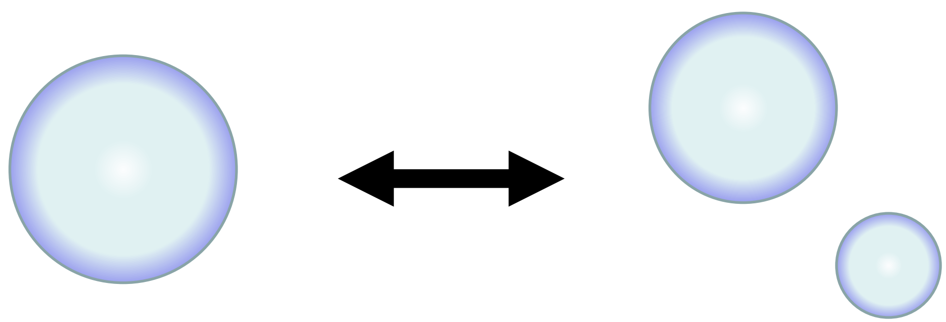

- Quantum tunneling and fluctuation

Time-dependent density functional theory (TDDFT) for nuclei

- Time-odd densities (current density, spin density, etc.)

$$E\left[\rho_q(t),\tau_q(t),\overleftrightarrow{J}_q(t),\vec{j}_q(t),\vec{s}_q(t),\vec{T}_q(t);\kappa_q(t)\right]$$

kinetic, spin-current, current, spin, spin-kinetic, pair density

- TD Kohn-Sham-Bogoliubov-de-Gennes eq.

$$i\frac{\partial}{\partial t}\begin{pmatrix} U_\mu(t) \\ V_\mu(t) \end{pmatrix} = \begin{pmatrix} h(t)-\lambda & \Delta(t) \\ -\Delta^*(t) & -\left(h(t)-\lambda\right)^* \end{pmatrix}\begin{pmatrix} U_\mu(t) \\ V_\mu(t) \end{pmatrix}$$

Decoupled submanifold

Klein, Do Dang, Walet, Phys. Rep. 335, 93 (2000)
Nakatsukasa, Prog. Theor. Exp. Phys. 2012, 01A207 (2012)

- Collective canonical variables (q,p)
  - $\{\xi^\alpha, \pi_\alpha\} \rightarrow \{q, p;\ q^a, p_a;\quad a = 2, \cdots, N_{ph}\}$
- Finding a decoupled submanifold Σ

$$\dot{q}^a = \left.\frac{\partial H}{\partial p}\right|_\Sigma \approx 0$$

$$\dot{p}^a = -\left.\frac{\partial H}{\partial q}\right|_\Sigma \approx 0$$

on the submanifold Σ

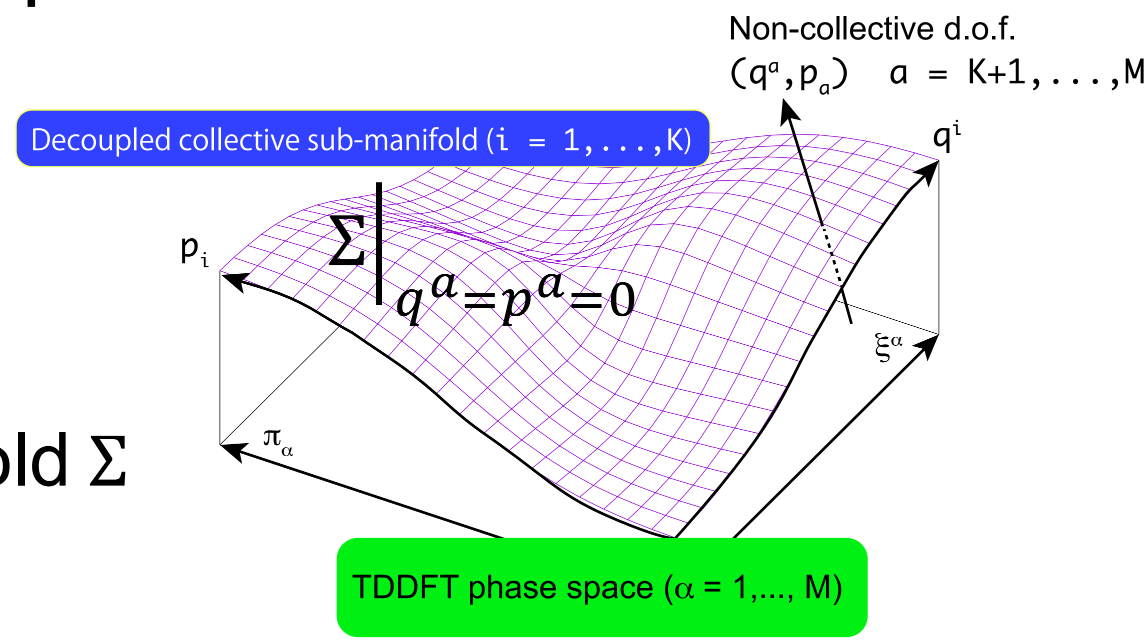

Numerical procedure

$$\frac{\partial V}{\partial \xi^{\alpha}} - \frac{\partial V}{\partial q}\frac{\partial q}{\partial \xi^{\alpha}} = 0$$

Moving mean-field eq.

$$B^{\beta\gamma}\left(\nabla_{\gamma}\frac{\partial V}{\partial \xi^{\alpha}}\right)\frac{\partial q}{\partial \xi^{\beta}} = \omega^{2}\frac{\partial q}{\partial \xi^{\alpha}}$$

Moving RPA eq.

Tangent vectors (Generators)

$$q_{,\alpha} = \frac{\partial q}{\partial \xi^{\alpha}} \qquad \xi^{\alpha}_{,q} = \frac{\partial \xi^{\alpha}}{\partial q}$$

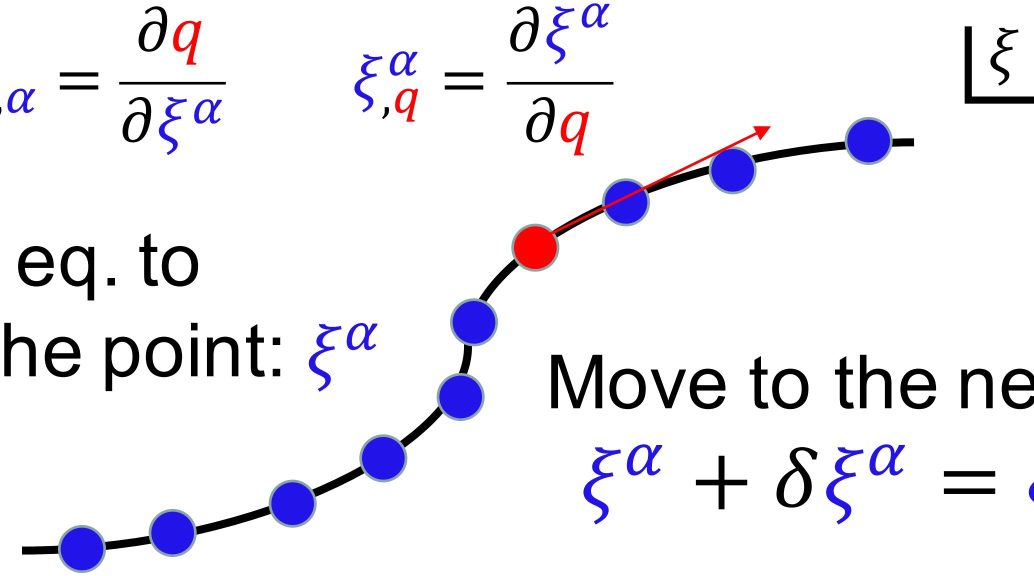

Moving MF eq. to determine the point: ξ^{α}

Move to the next point

$$\xi^{\alpha} + \delta\xi^{\alpha} = \xi^{\alpha} + \varepsilon\xi^{\alpha}_{,q}$$

3D real space representation

- 3D space discretized in lattice
- BKN functional: $E_{\mathrm{BKN}}[\rho, \tau]$ (*rather schematic*)
- Moving mean-field eq.: Imaginary-time method
- Moving RPA eq.: Finite amplitude method (PRC 76, 024318 (2007))

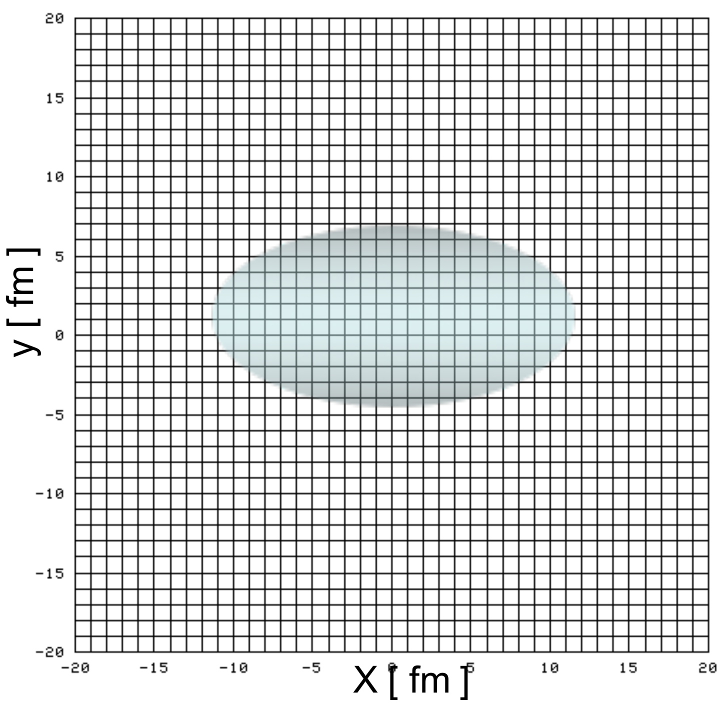

At a moment, no pairing

1-dimensional reaction path extracted from the Hilbert space of dimension of $10^4 \sim 10^5$.

Simple case: α + α scattering

α particle (^4He)　　α particle (^4He)

- Reaction path
- After touching
  - No bound state, but
  - a resonance state in ^8Be

^{8}Be: Tangent vectors (generators)

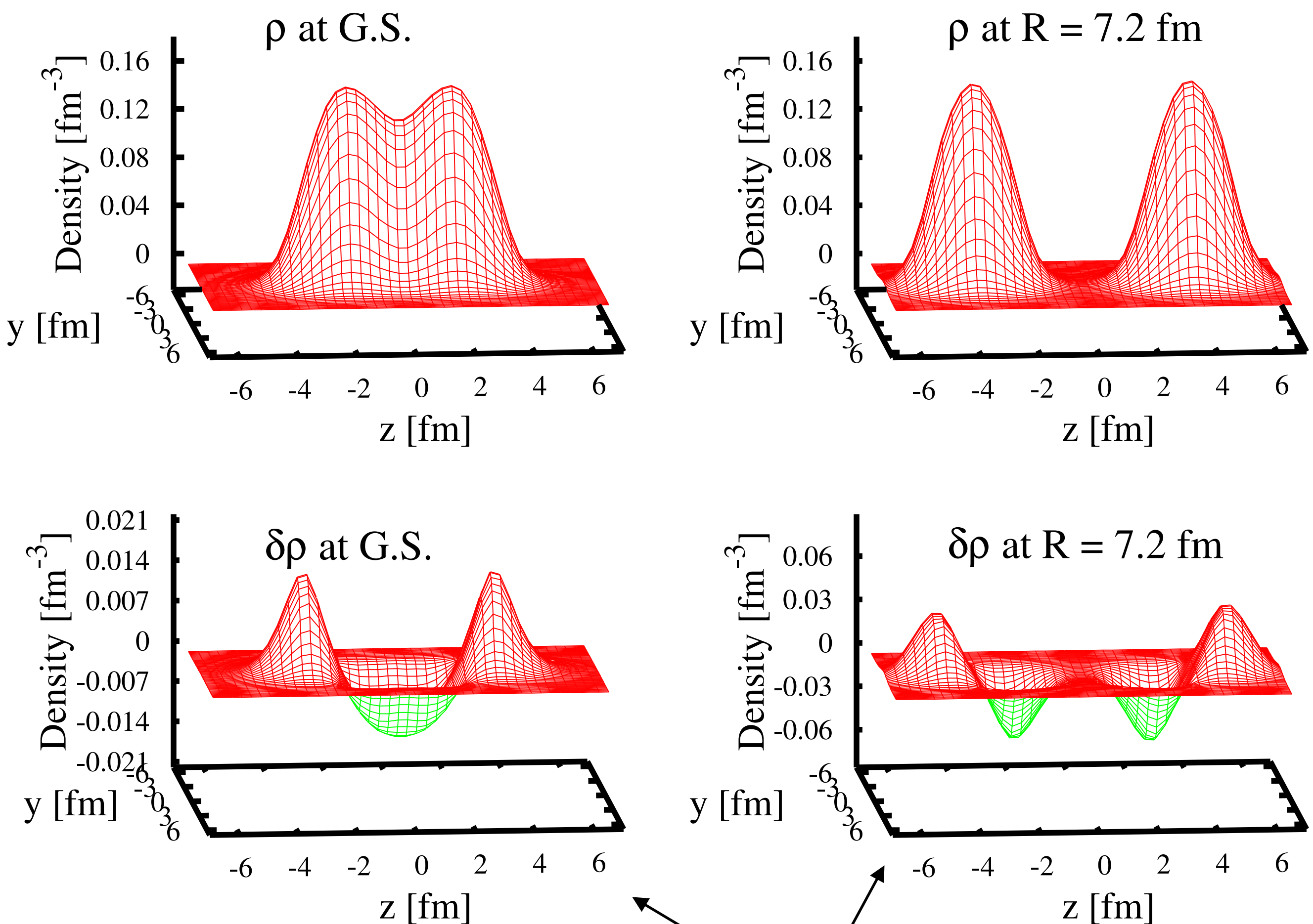

$\rho(\vec{r})$

$\delta\rho(\vec{r})$

Tangent vectors (Generators)

α + α scattering (phase shift)

Wen, T.N., PRC 94, 054618 (2016).

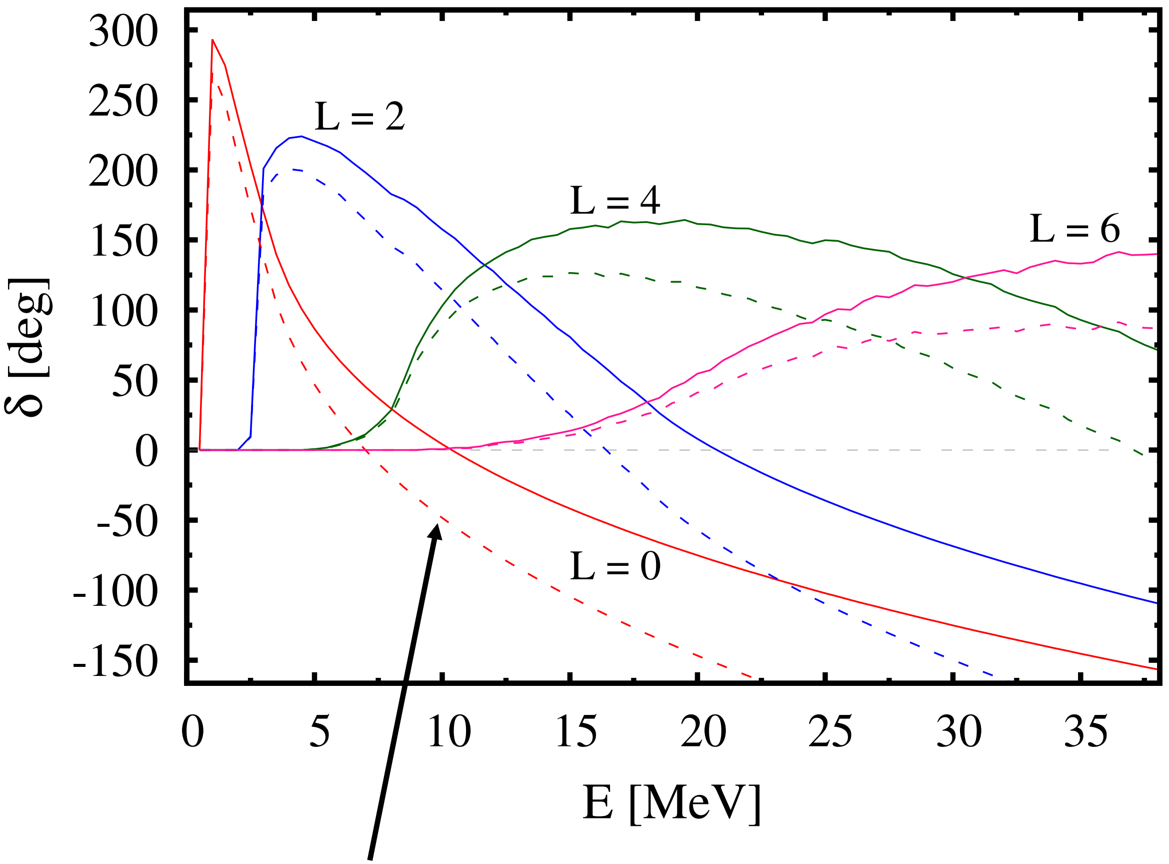

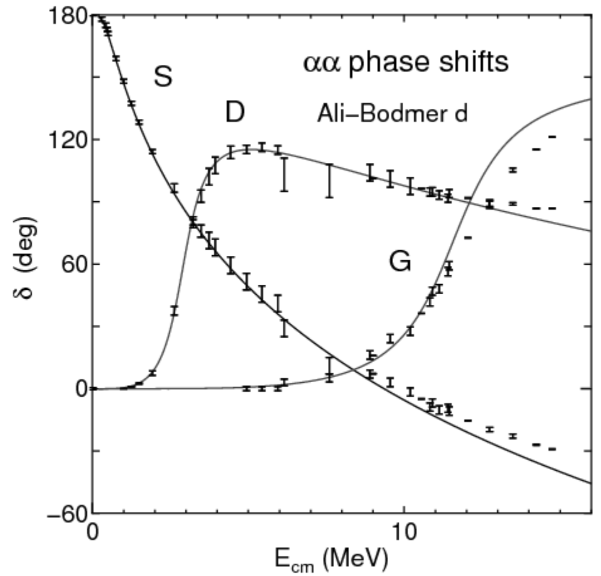

Effect of dynamical change of the inertial mass

Dashed line: Constant reduced mass ($M(R) \rightarrow 2m$)

$^{16}O+^{16}O \rightarrow ^{32}S$: Reaction path

Wen, T.N., PRC 96, 014610 (2017).

Starting from two ^{16}O configuration

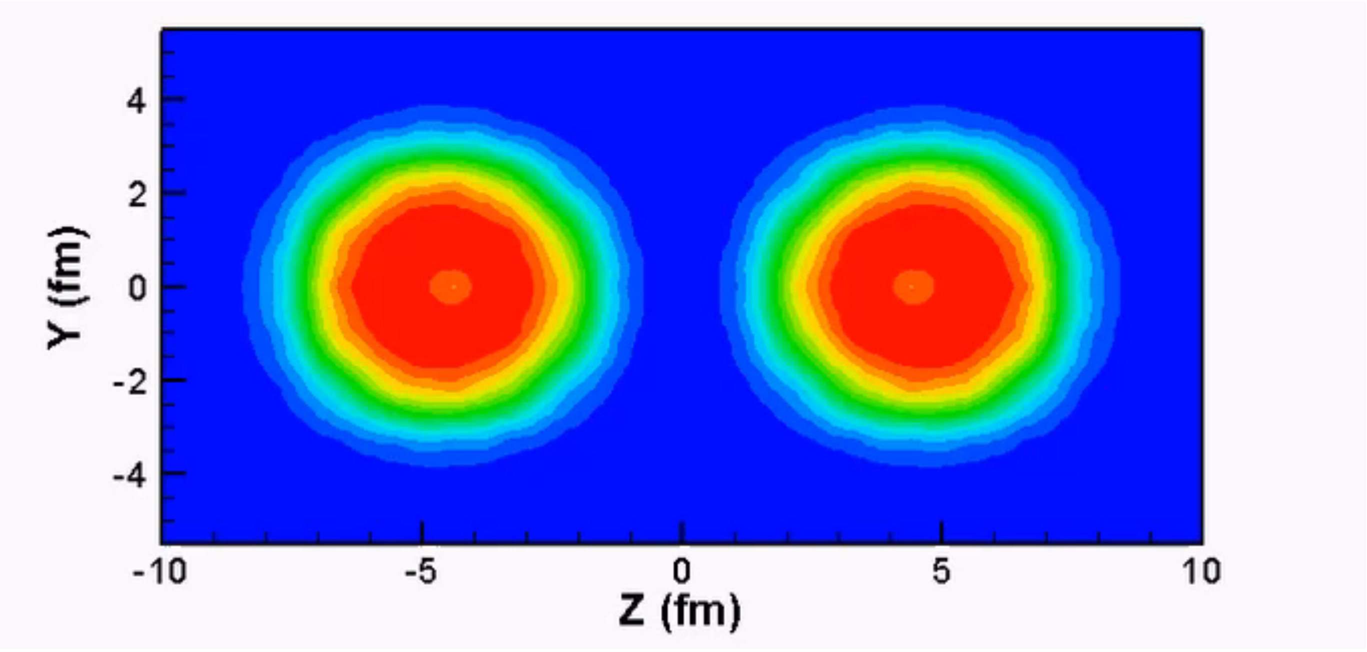

$^{16}O + ^{16}O \rightarrow ^{32}S$: Collective potential

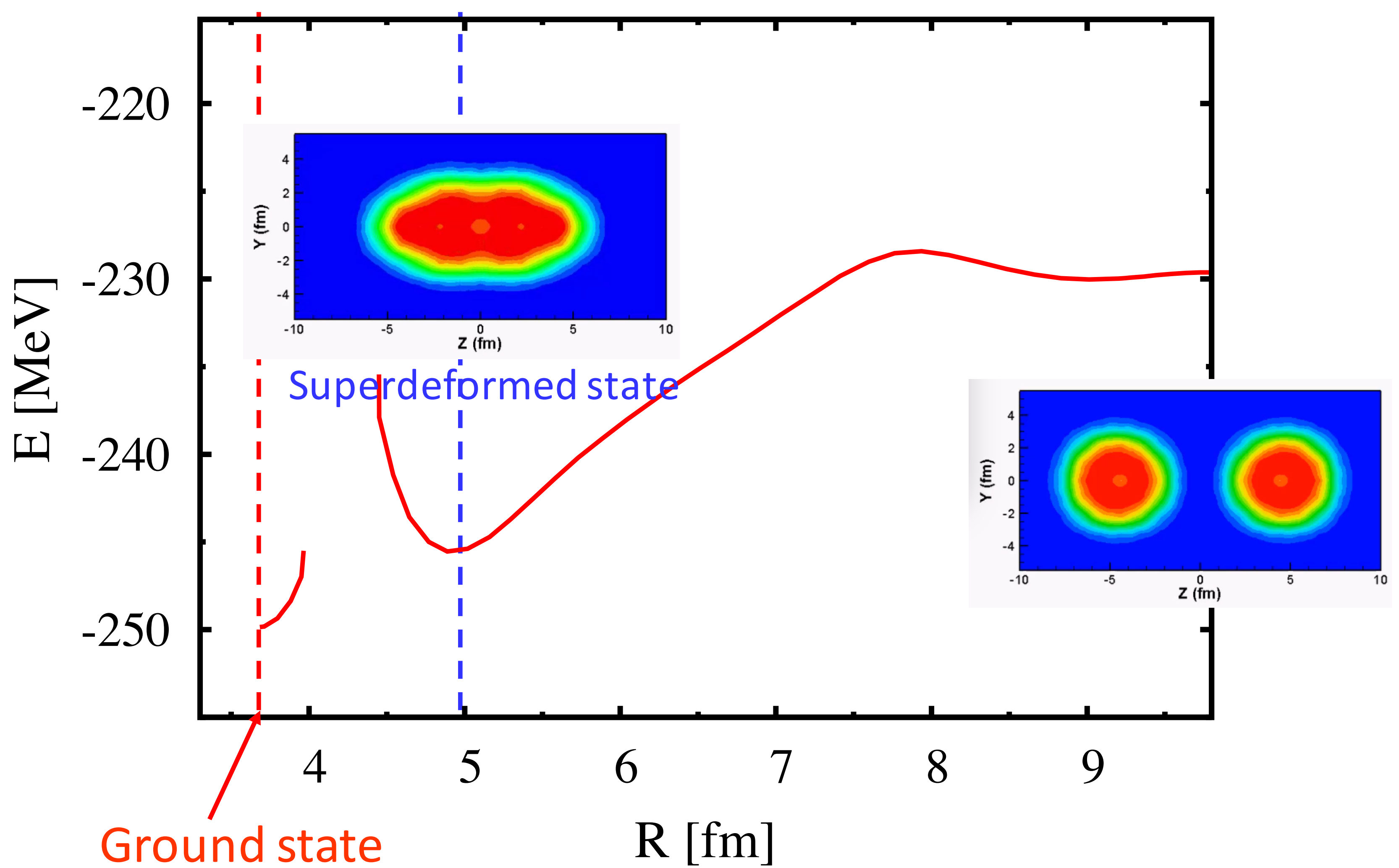

$^{16}O+^{16}O \rightarrow {}^{32}S$: Collective mass

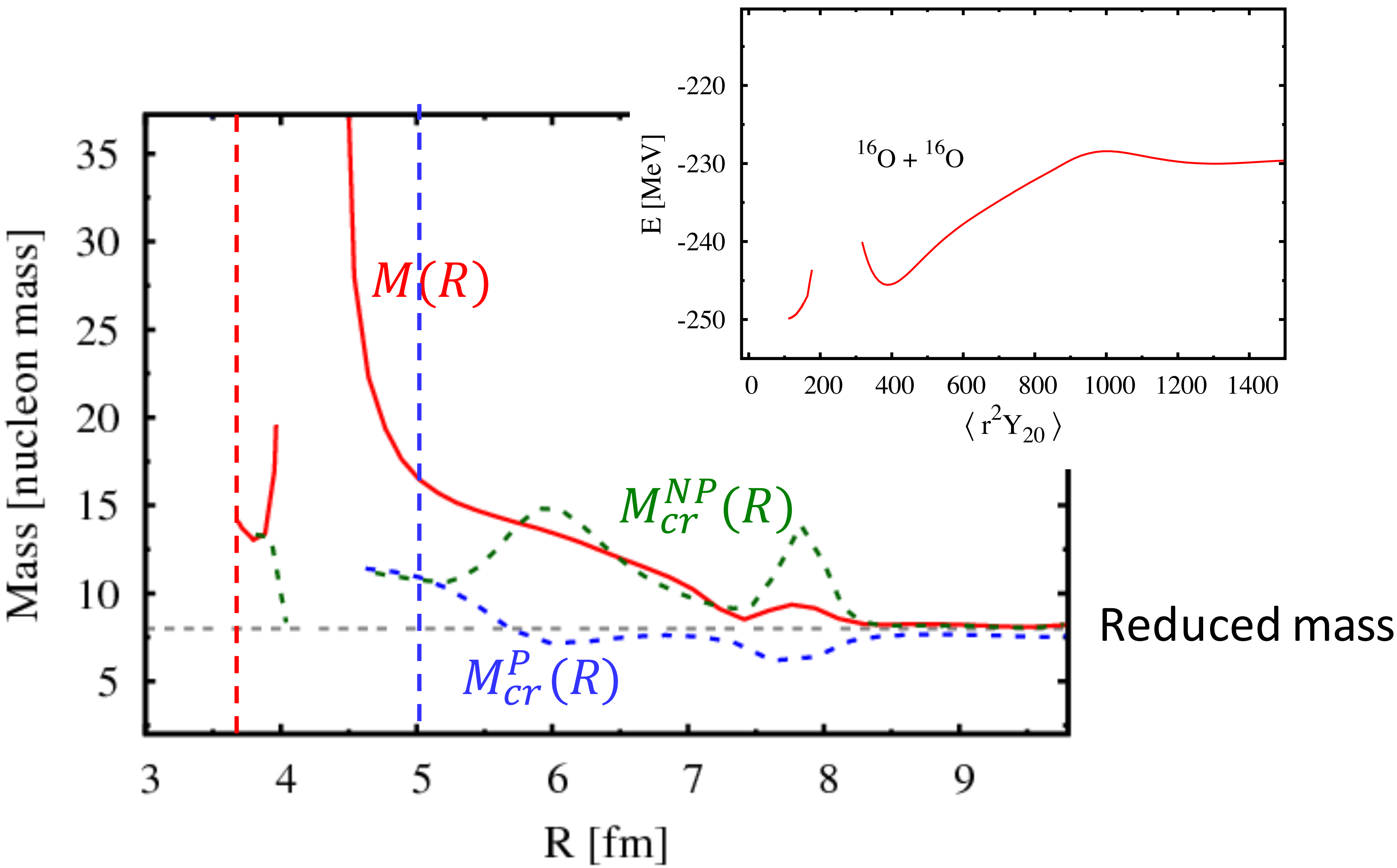

Fusion reaction: $^{16}O + ^{16}O$

Effect of dynamical change of the inertial mass *hinders the fusion cross section by 2 orders of magnitude*.

Exp (Ni+Ni)

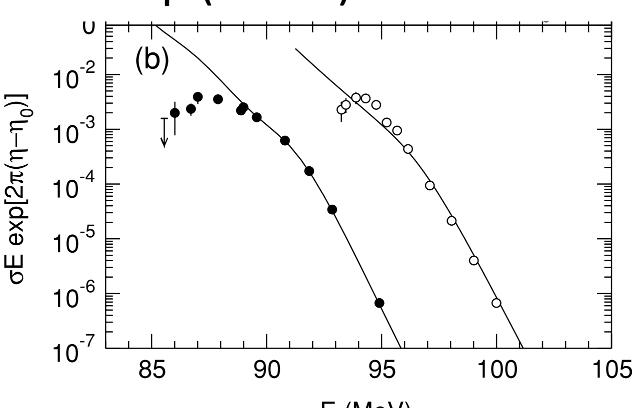

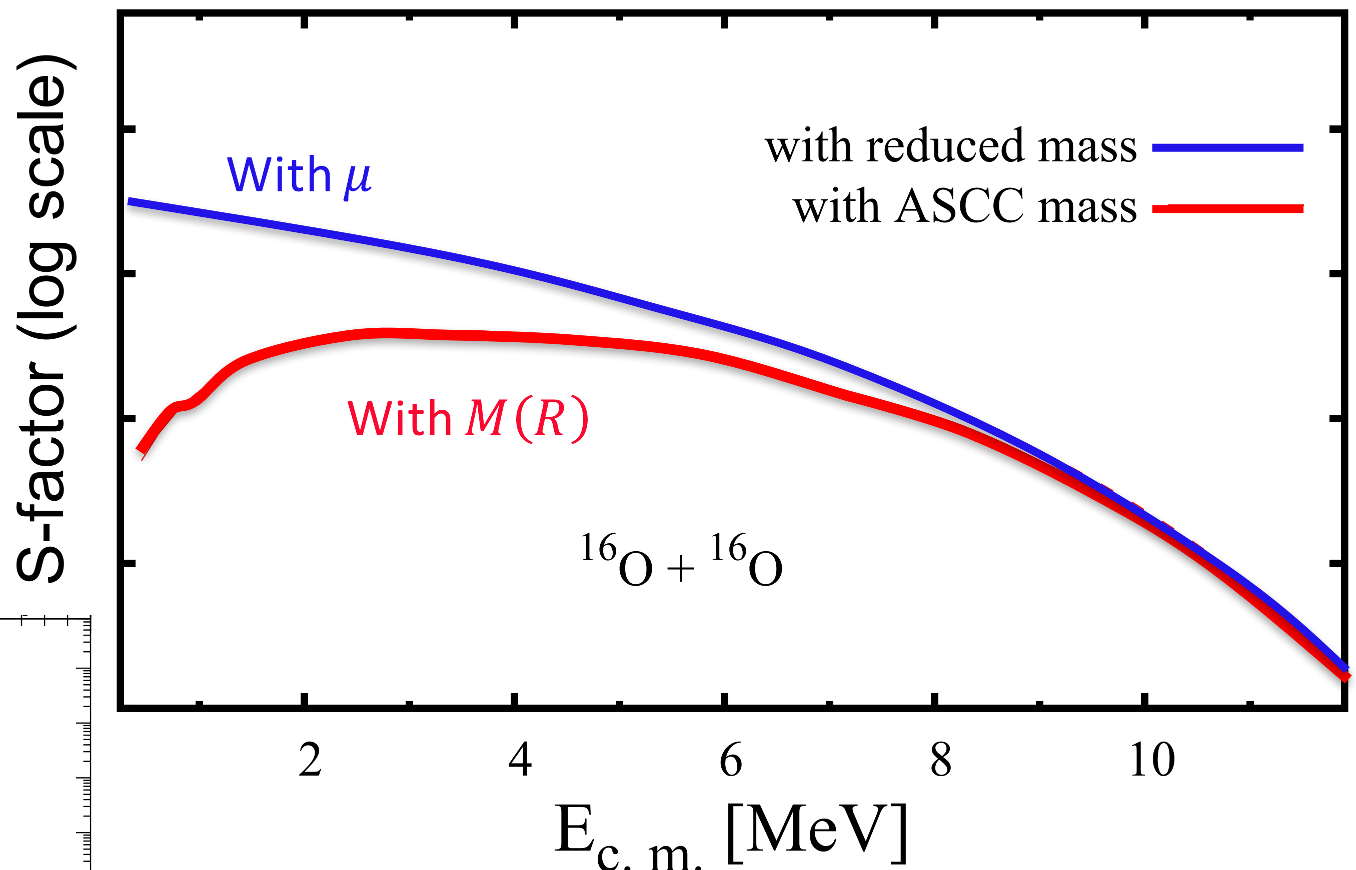

Summary (Addressed questions)

- Quantum clusters and reaction
  - What kind of clusters? What kind of reaction path?
  - How to incorporate quantum effect (fluctuations)?
  - Velocity-dependent and spin-orbit effect?
  - Excess neutrons effect on reaction dynamics?
  - Effect of superfluidity?
- Inhomogeneous nuclear matter
  - Neutrons' mobility and pulsar glitch crisis?
  - Effect of superfluidity?